A Foot-mounted PDR System Based On IMU/EKF+HMM+ZUPT+ZARU+HDR+Compass Algorithm

Wenchao Zhang[1,2], Xianghong Li[1,2] , Dongyan Wei[2], Xinchun Ji[2], Hong Yuan[2]
1. University of Chinese Academy of Sciences
2. Academy of Opto-electronics, Chinese Academy of Sciences
Beijing, China
Correspondence Email: weidongyan@aoe.ac.cn

Abstract—A foot-mounted pedestrian dead reckoning system is a self-contained technique for indoor localization. An inertial pedestrian navigation system includes wearable MEMS inertial sensors, such as an accelerometer, gyroscope, barometer, or magnetometer, which enable the measurement of the step length and the heading direction. In this plan, a method based on IMU/EKF+HMM+ZUPT+ZARU+HDR+the Earth Magnetic Yaw was designed to realize foot-mounted pedestrian navigation. Based on the characteristics of pedestrian navigation, the general likelihood ratio test (GLRT) and the Hidden Markov Model (HMM) were used to realize the detection of zero speed interval at different speed states. When the zero speed state is detected, the zero velocity update (ZUPT) method is used to limit the accumulation of IMU. The Zero Angular Rate Update (ZARU) + (heuristic heading reduction) HDR+the Earth Magnetic Yaw method is used to limit the IMU attitude and heading drift. Finally, the EKF method is used to realize the effective estimation and feedback of the speed, attitude and heading error of the pedestrian navigation system. Meanwhile, a fault detection algorithm based on the innovation vector is added to the EKF system to effectively detect and eliminate the gross errors in the measurements, to improve the filtering effect of EKF algorithm, and ensure the accuracy of pedestrian navigation results.*

Keywords—GLRT; HMM; ZUPT; ZARU; HDR; the Earth Magnetic Yaw; EKF; fault detection algorithm

I. INTRODUCTION

A wide range of different sensor technologies have been developed for pedestrian location systems, which can be classified in two categories: infrastructure-based and infrastructure-less systems. Infrastructure-based positioning systems need infrastructure such as electrical power, internet access, or walls for reference points mounting [1]. In contrast, infrastructure-less positioning systems such as dead reckoning or image based systems do not require any infrastructure, which can be used in any kind of indoor environment [13].

Infrastructure-less method for person's localization are mainly based on Pedestrian Dead Reckoning (PDR) by using foot mounted inertial sensors [2]-[5]. The used Micro Electro-Mechanical System (MEMS) inertial sensors are accelerometer, gyroscope, or digital compass, which enable the measurement of the step length and the heading direction. Since the inertial sensors suffer from drift, which accumulates over time, the position and velocity errors grow with time. Zero Angular Rate Update (ZARU) is a technique that can help estimating the bias of the gyroscope in every still phase [6]. Borenstein et al. [7] proposed a technique called Heuristic Drift Reduction (HDR) to reduce the heading error, which is based on the assumption that most of the corridors and paths inside a building are straight. Another approach to minimize the positioning errors is the Zero Velocity Updates (ZUPT), which is a most common method and assumes that during walking, the foot touches the ground and remains stationary for a short time (stance phase) [2].

In this plan, some general work from Luan Van Nguyen et al. [8] and A.R. Jim enez et al. [9] is followed. But, the three main different contributions of the plan are the following: 1) development of a dynamic gait phase detection algorithm, which combined the GLRT [10] with the HMM [11], for accurate detection of human foot gait phases(swing and stance) in dynamic speeds, such as walking and running[12]; 2) development of a real-time and accurate foot motion localization algorithm, which can integrate the ZUPT, ZARU, HDR, The Earth Magnetic Yaw and EKF to address IMU drift in the pedestrian navigation. 3) In the EKF system, a fault detection algorithm based on the innovation vector is added, which can real-time effectively detects and removes the possible gross errors in the measurements, to improve the filtering effect of the EKF algorithm, and ensures the accuracy of the foot-mounted pedestrian navigation results.

II. OVERVIEW OF THE HUMAN FOOT-MOUNTED PDR SCHEME

The overview of the human foot-mounted PDR scheme, with three different modules, is shown in Fig. 1.

The bottom module is an IMU device with four sensors: an accelerometer for measuring acceleration a_{t+1}^b, a gyroscope for measuring angular rate ω_{t+1}^b , a magnetometer for measuring magnetic field of the Earth o_{t+1}^b, and a barometer for measuring barometric pressure of the Earth, using which the person's
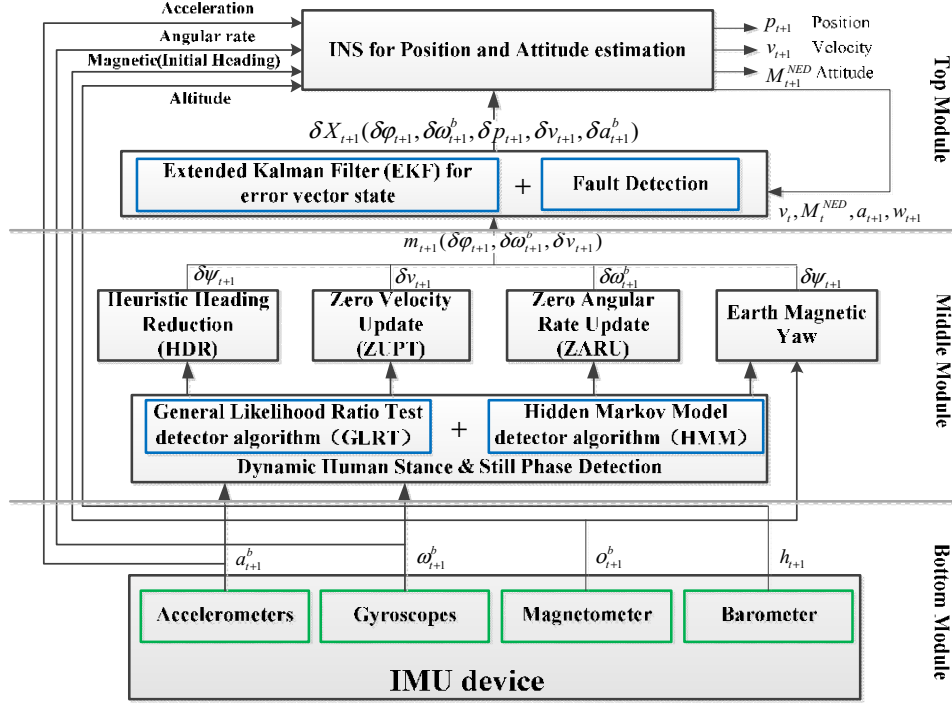
Fig.1. The Scheme of IMU/EKF+HMM+ZUPT+ZARU+HDR+Compass algorithm

altitude h_{t+1} can be calculated. The superscript b in these formulas refers to the value of these variables in the body frame of the IMU device; the subscript $t+1$ refers to the value of these variables at discrete time $t+1$ in the IMU's time series, as shown in Fig. 2.
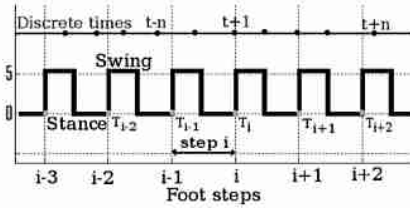

Fig.2. The discrete time of IMU's time series and corresponding foot steps

The middle module includes five components: the Stance & Still Phase Detection, the HDR, the ZUPT, the ZARU, and the Earth Magnetic Yaw. Meanwhile, the Stance & Still Phase Detection includes two components: the GLRT detector algorithm [10] used under the condition of the slow and normal pedestrian gait speed, and the HMM detector algorithm [11] used under the condition of the dynamic and fast pedestrian gait speed, such as fast walking. When the Stance & Still Phase Detection detects the stance and swing phases of human foot gait from IMU's data, the HDR, the ZUPT, the ZARU, and the Earth Magnetic Yaw utilize these data to estimate the error vector $m_{t+1}(\delta\psi_{t+1}, \delta\omega_{t+1}^b, \delta v_{t+1})$ (see Fig.1), where $\delta\psi_{t+1}$, $\delta\omega_{t+1}^b$ and δv_{t+1} denotes the bias error of yaw, the bias error of angular rate and the bias error of velocity at time $t+1$, respectively. $m_{t+1}(\delta\psi_{t+1}, \delta\omega_{t+1}^b, \delta v_{t+1})$ is the most important input data for the success of the EKF algorithm. Because the EKF requires

kinematically related measurements of position, velocity, and attitude, it has to rely on the supports from the Stance & Still Phase Detection, the HDR, the ZUPT, the ZARU and the Earth Magnetic Yaw.

The top module includes an INS and an EKF. The INS system alone can't cope with the IMU drift. The EKF, with a properly constructed sensor fusion, can estimate the IMU biases. Therefore, it can help the INS in reducing the IMU drift. The EKF estimates the errors of actual acceleration, velocity, and position of human foot motion, by taking the measurement error vector from the middle module and the feedback data from the output of the INS (see Fig.1). On its turn, the INS receives IMU's data and the state measurement errors δX_{t+1} from the EKF to continuously compute, via dead reckoning, the velocity, attitude, and position of human foot motion.

III. THE HUMAN FOOT-MOUNTED PDR ANALYSIS

A. Stance & Still Phase Detection

A gait or a walk cycle consists of two phases: the swing and stance phase. In the swing phase, the foot is not in contact with the ground. In contrast, the foot contacts the ground in the stance phase.

The GLRT detector algorithm proposed in [10] has obvious advantages for zero velocity interval detection of stable pedestrian gait velocity, which using both the specific force vector a_{t+1}^b and the angular rate vector ω_{t+1}^b from the IMU. The objective of the zero-velocity interval detector is to determine whether the IMU is moving or stationary, given the measurement sequences $z_{t+1}^a \triangleq \{a_k\}_{k=t+1}^{t+W}$ and

$z_{t+1}^w \triangleq \{w_k\}_{k=t+1}^{t+W}$. Here, W denotes the window size of the zero-velocity detector. Mathematically, if the IMU is stationary, then

$$T\left(z_{t+1}^a, z_{t+1}^w\right) < \gamma \qquad (1)$$

Here, $T\left(z_{t+1}^a, z_{t+1}^w\right)$ are the test statistics of the detector and γ is the detection threshold. The GLRT detector is described as follows:

$$T\left(z_{t+1}^a, z_{t+1}^w\right) = \frac{1}{W} \sum_{k=t+1}^{t+W} \left(\frac{1}{\sigma_a^2} \left\| a_k - g \frac{\bar{a}_{t+1}}{\|\bar{a}_{t+1}\|} \right\|^2 + \frac{1}{\sigma_w^2} \|w_k\|^2 \right) \qquad (2)$$

Here, σ_a^2 and σ_w^2 denote the variance of the measurement noise of the accelerometers and gyroscopes, respectively. And, $\|a\| = a^T a$, where $(\cdot)^T$ denotes the transpose operator. $\bar{a}_{t+1}$ denotes the sample mean, i.e.,

$$\bar{a}_{t+1} = \frac{1}{W} \sum_{k=t+1}^{t+W} a_k \qquad (3)$$

While the HMM detector algorithm proposed in [11] has a good effect for zero velocity interval detection of dynamic and fast pedestrian gait speed, which separates the dominant rotation axis gyroscope output into a series of segments and these segments are modeled as output processes of a hidden Markov model. For example, when the y-axis is the dominant rotation axis, the y-axis gyroscope output can be divided into four repetitive segments as follows:
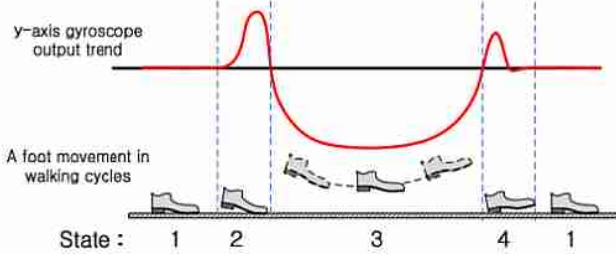

Fig.3. The four typically repetitive segments in normal walking cycles

As shown in Fig.3, the state 1 is a zero velocity interval. Each segment in the walking cycle can be identified by using the finite state hidden Markov model. We assume that there is a Markov process X_i and X_i is assumed one of four states: 1, 2, 3 and 4. When a person is walking or running, a typical state transition is $1 \to 2 \to 3 \to 4 \to \cdots$. The Markov process X_i is estimated through the output Y_i (that is, the y-axis gyroscope output segment).

By a trial-and-error process of the dynamic walking and running cycle, the state transition matrix A of the observation matrix C (which represents the link between the output Y_i and the state process X_i) of the HMM can be obtained.

$$A_{mn} = \Pr[X_{k+1} = m \mid X_{k+1} = n] \qquad (4)$$

$$C_{mn} = \Pr[Y_k = m \mid X_k = n] \qquad (5)$$

Here, (m,n) denotes (m,n)-th element of A or C.

Once A and C are defined, Markov process state X_i can be estimated from the output Y_i using HMM filters. Then the state 1 can be identified, which is the zero velocity interval.

Thus, we combine the two methods to achieve the dynamic human stance & still phase detection (See Fig.4).
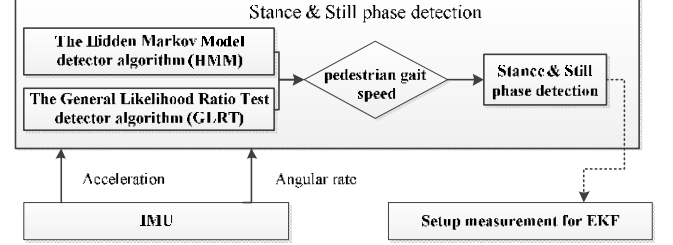

Fig.4. Stance & Still detection block

The GLRT detector algorithm is used under the condition of the slow and normal pedestrian gait speed, while the HMM detector algorithm is used under the condition of the dynamic and fast pedestrian gait speed, such as fast walking or running.

B. The EKF algorithm

The IMU/EKF+HMM+ZUPT+ZARU+HDR+Compass algorithm is shown in Fig.5. The error state vector[2],[9] at time $t+1$ is a 15-element vector:

$$\delta X_{t+1}(\delta\varphi_{t+1}, \delta\omega_{t+1}^b, \delta p_{t+1}, \delta v_{t+1}, \delta a_{t+1}^b) \qquad (6)$$

Where $\delta\varphi_{t+1}$, $\delta\omega_{t+1}^b$, δp_{t+1}, δv_{t+1} and δa_{t+1}^b represent the EKF's estimated errors of attitude, angular rate, position, velocity, and acceleration at time $t+1$, respectively. And its function corrects the INS's output values: the velocity, the position, and the attitude.
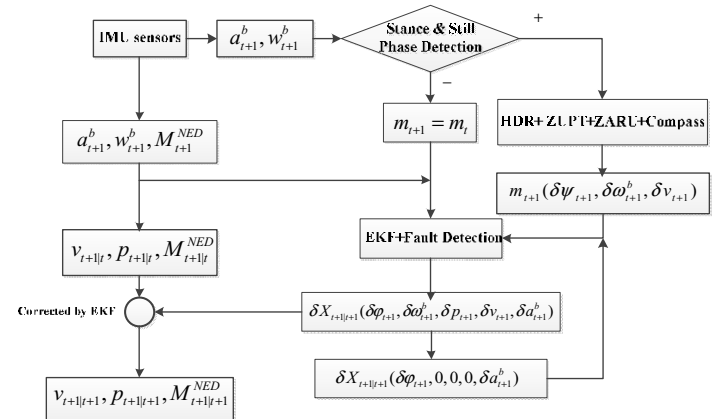

Fig.5. the IMU/EKF+HMM+ZUPT+ZARU+HDR+Compass algorithm

When incorporating the HDR, ZUPT, ZARU and Compass, the measurement error vector m_{t+1} is as follows:

$$m_{t+1} = \left[\delta\psi_{t+1}, \delta w_{t+1}^b, \delta v_{t+1}^b \right] \tag{7}$$

Where $\delta\psi_{t+1}$, $\delta\omega_{t+1}^b$ and δv_{t+1} denote the bias error of yaw, the bias error of angular rate and the bias error of velocity at time $t+1$, respectively. And the measurement matrix H must be:

$$H_{7\times15} = \begin{bmatrix} [001] & 0_{1\times3} & 0_{1\times3} & 0_{1\times3} & 0_{1\times3} \\ 0_{3\times3} & I_{3\times3} & 0_{3\times3} & 0_{3\times3} & 0_{3\times3} \\ 0_{3\times3} & 0_{3\times3} & 0_{3\times3} & I_{3\times3} & 0_{3\times3} \end{bmatrix} \tag{8}$$

C. Fault detection algorithm

In the EKF algorithm, $r_{t+1} = Z_{t+1} - H_{t+1}X_{t+1|t}$ is called the innovation vector at time $t+1$. For the possible gross errors in the measurements, the method based on the innovation vector can effectively detect and remove the gross errors to ensure the accuracy of the measurements. If there's no gross exists, r_{t+1} can be approximated by the second order AR model:

$$r_{t+1} = a_1 r_t + a_2 r_{t-1} + w_{t+1} \tag{9}$$

where, w_{t+1} denotes the zero mean white noise sequence. In order to remove the effects of noise, take the mean of the innovation vector:

$$S_{t+1} = \frac{1}{t+1}\sum_{i=1}^{t+1} r_i = \frac{1}{t+1}\sum_{i=1}^{t+1}(a_1 r_i + a_2 r_{i-1} + w_{i+1}) \tag{10}$$

Since the mean of w_{i+1} is zero sequence, if $t+1$ is a large value, there is $\frac{1}{t+1}\sum_{i=1}^{t+1} w_{i+1} = 0$. So make $\mu_{t+1} = \frac{S_{t+1} - S_t}{S_t - S_{t-1}}$, if no gross errors exist, $\mu_{t+1} \approx 1$, while gross errors exist in the measurements, the $\mu_{t+1} \approx 1$ is invalid. By calculating the deviation of μ_{t+1} from the mean, then using the 3σ criteria to detect and remove the gross errors.

IV. EXPERIMENTAL EVALUATION

In this section, the proposed algorithm is implemented in the indoor experiment, in order to evaluate the accuracy of the position estimation of the foot-mounted PDR system.

A. Hardware Description

We use the MTi-100 IMU device from Xsens Technologies B.V (Enschede, The Netherlands).The IMU has three orthogonally-oriented accelerometers, three gyroscopes, three magnetometers and a barometer. The specifications of this IMU are presented in tables I. In the experiment, the MTI-100 device is fixed on the foot surface (See Fig.6). At the beginning of the data acquisition, the foot should be kept still for a while to implement the initial alignment of IMU, then, the dynamic human foot-mounted PDR experiment can be carried out.

TABLE I   SPECIFICATION OF MTI-100

Specification	Acceleration	Gyroscope	Magnetometer	Barometer
Full Range	50m/s²	±450°/s	±80uT	300-1100hPa
Bias stability	40ug	10°/h	N/A	N/A
Bandwidth(-3dB)	375Hz	415 Hz	N/A	N/A
Noise density	80 ug $/\sqrt{Hz}$	0.01°/s $/\sqrt{Hz}$	200uG $/\sqrt{Hz}$	0.01hPa $/\sqrt{Hz}$

Fig.6. MTI-100 attached to the foot

B. The indoor experiment route line

The Fig.7 is the data acquisition route trajectory, point 1 is the starting point whose coordinate is (0, 0, 0) and the coordinate system can be established. Floor5, Floor 6, Floor 7 and Floor 8 are floors of the experiment building. C1, C2, C3 and C4 are the space beside every floor's elevator (4.8m*7.2m), respectively. S1, S2 and S3 are the stairs between the floors. The coordinates of point 1 to 14 are known, and the starting point 1 coincides with the end point 14 on the projection plane. Similarly, the corresponding points of each floor coincide with each other on the projection plane, for example, points 2, 5, 10 and 13 are coincident on the projection plane. The experimental route line is as follow: Start from the Floor 5th's point 1, walk along the floor to collect data with dynamic speed, go around in C1 for once time, and take the stairs through the floor, the same way as the other floors, finally reach the Floor 8th's point 14. The total length of the route line is about 310m. The experiment repeats for three times.
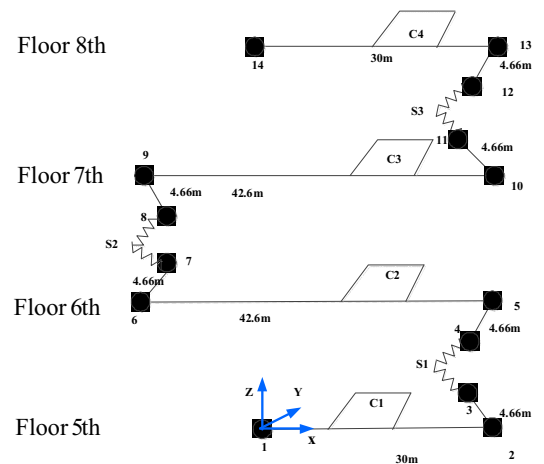

Fig.7. the indoor experiment route line

C. The evaluation method

By comparing the calculated coordinates of Point 2, 5, 6, 9, 10, 13 with the reference coordinates, the points' plane error can be obtained. The route line plane closed error can be obtained by comparing the plane coordinates of Point 1 with Point 14. The error/length can be obtained by using the closed error divides the length of the route line.

D. The experiment result

One of the experimental data result is shown in Fig.8. and Fig.9. The Plane error assessment results of the three group test data are shown in table II.
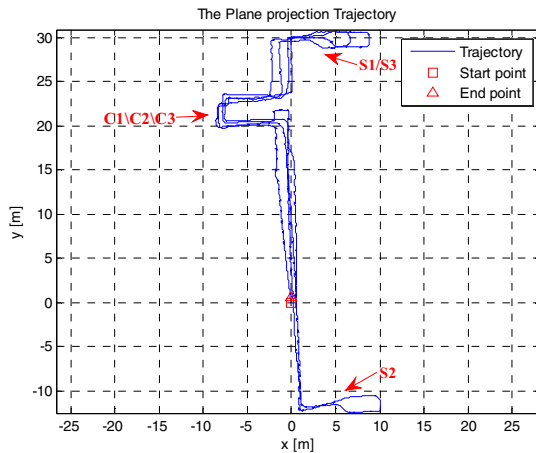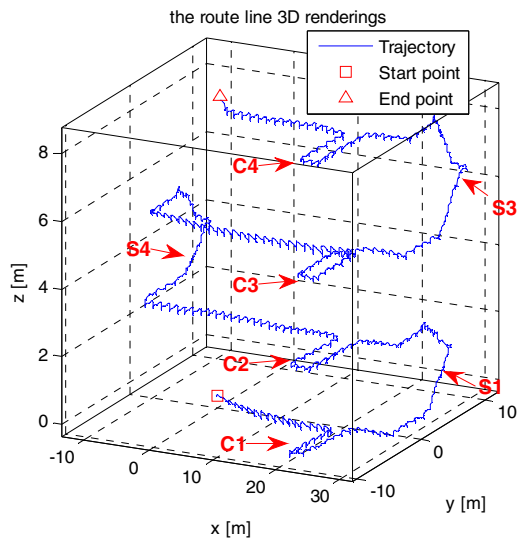

Fig.8. Route line Plane projection

Fig.9. Route line 3D renderings

TABLE II   Route line plane error assessment results

Point No.	Point 2	Point 5	Point 6	Point 9	Point 10	Point 13	Closed error	Error/ length
Plane error1(m)	0.160	0.248	0.452	0.483	0.576	0.616	0.672	0.217%
Plane error2(m)	0.301	0.410	0.603	0.688	0.797	0.759	1.084	0.350%
Plane error3(m)	0.182	0.205	0.324	0.342	0.451	0.502	0.643	0.207%

E. Discussion

We have evaluated our algorithm in the real indoor environment. The experiment shows that the algorithm can effective eliminate the error accumulation of the IMU device, with a high accuracy.

REFERENCES

[1] R. Mautz, "Indoor positioning technologies," M.S. thesis, Dept. Civil,Environ. Geomatic Eng., Inst. Geodesy Photogram., Zürich, Switzerland,2012.

[2] E. Foxlin, "Pedestrian tracking with shoe-mounted inertial sensors,"IEEE Comput. Graph. Appl., vol. 25, no. 6, pp. 38–46, Nov. 2005

[3] S. Godha and G. Lachapelle, "Foot mounted inertial system for pedes-trian navigation," Meas. Sci. Technol., vol. 19, no. 7, p. 075202, 2008.

[4] D. Caspari, L. Riedhammer, M. Strutu, and U. Grossmann, "Smartphone sensor based algorithms for dead reckoning using magnetic field sensor and accelerometer for localization purposes," inProc. 2nd Int. Symp. Wireless Syst. Conf. Intell. Data Acquisition Adv. Comput. Syst., Technol. Appl. (IDAACS-SWS), Sep. 2014, pp. 66–72.

[5] X. Yun, E. R. Bachmann, H. Moore, and J. Calusdian, "Self-contained position tracking of human movement using small inertial/magnetic sensor modules," in Proc. IEEE Int. Conf. Robot. Autom., Apr. 2007,pp. 2526–2533.

[6] A. R. Jiménez, F. Seco, J. C. Prieto, and J. Guevara, "Indoor pedestrian navigation using an INS/EKF framework for yaw drift reduction and a foot-mounted IMU," in Proc. 7th Workshop Positioning Navigat. Commun. (WPNC), Mar. 2010, pp. 135–143

[7] J. Borenstein, L. Ojeda, and S. Kwanmuang, "Heuristic reduction of gyro drift for personnel tracking systems,"J. Navigat., vol. 62, no. 1, pp. 41–58, 2009

[8] Luan Van Nguyen and Hung Manh La, "Real-Time Human Foot Motion Localization Algorithm With Dynamic Speed", IEEE Transcations on human-machine system, vol. 46, no. 6,2016.

[9] A. R. Jimenez, F. Seco, J. C. Prieto, and J. Guevara, "Indoor pedestrian navigation using an INS/EKF framework for yaw drift reduction and a foot-mounted IMU,"Proc. 7th Workshop IEEE Positioning Navigat. Commun., 2010, pp. 135–143.

[10] Isaac Skog, Peter H¨andel, Senior Member . Zero-velocity detection—an algorithm evaluation[J]. IEEE Transactions On Biomedical Engineering, vol. 57, no. 11,2010.

[11] Sang Kyeong Park and Young Soo Suh. A Zero Velocity Detection Algorithm Using Inertial Sensors for Pedestrian Navigation Systems[J]. Sensors,2010(10):9163-9178.

[12] Tang Wengjie, "Reaserch on Pedestrian Navigation Aglorithm Based on MIMU"[D].Zhengzhou, PLA Information Engineering University,2016.

[13] Abdelmoumen Norrdine, Zakaria Kasmi, and Jörg Blankenbach, "Step Detection for ZUPT-Aided Inertial PedestrianNavigation System Using Foot-Mounted Permanent Magnet" [J].IEEE Sensors vol. 16, no. 17,2016.